Supporting Information for

Enhancing visual fluorescence detection of tetracycline antibiotics through regulation of nitrogen-containing ligand and antenna effect of Ln^{3+}

Tingting Liu[a], Mengna Ji[a], Jun Zheng[a], Nana Liu[a], Hongguo Hao[a], Jianmin Dou[a], Jingjing Jiang[b], Yunwu Li[a]*, Suna Wang[a]*

[a] Shandong Provincial Key Laboratory of Chemical Energy Storage and Novel Cell Technology, School of Chemistry and Chemical Engineering, Liaocheng University, Liaocheng, 252059, P. R. China

[b] Institute of Analysis and Testing, Beijing Academy of Science and Technology (Beijing Center for Physical and Chemical Analysis), Beijing 100094, P. R. China

Email: liyunwu@lcu.edu.cn; wangsuna@lcu.edu.cn

Table of Content

Table S1. Crystal structure data and refinement parameters of **LCU-127** and **LCU-128**.

Table S2. Selected bond lengths [Å] and angles [º] for **LCU-127** and **LCU-128**.

Table S3. The reported CPs/MOFs as sensors for TC detection.

Fig. S1 (a) and (c) Coordination mode of H_3L in **LCU-127** and **LCU-128**, respectively. (b) and (d) Coordination mode of ttytb and tpytz n **LCU-127** and **LCU-128**, respectively. (e) and (f) Stacking interactions of **LCU-127** and **LCU-128** between adjacent layers, respectively.

Fig. S2 (a) and (b) PXRD spectra of **LCU-127** and **LCU-128** after soaking in H_2O and different pH solutions, respectively**.** (c) and (d) PXRD spectra of **LCU-127** and **LCU-128** after soaking in different organic solvents for three days, respectively.

Fig. S3 TG of **LCU-127** and **LCU-128**, respectively.

Fig. S4 (a) Solid-state emission spectra and (b) CIE coordinates of **LCU-127** and **LCU-128**.

Fig. S5 (a) The detection limit calculation and (b) time-dependent response of **LCU-128** toward TC.

Fig. S6 (a) and (b) The luminescence intensity of **LCU-128** suspensions of common cations, anions, and some common organic matters with and without TC, respectively.

Fig. S7 (a)-(g) Luminescence intensity of **LCU-128** toward TC in NaCl, Na_2SO_4 solutions, temperature at 0 °C and room temperature (25 °C) and pH at 5, 6, 8, and 9, respectively.

Fig. S8 (a) and (c) Emission spectra of **LCU-128** dispersed in NaCl and Na_2SO_4 upon incremental addition of TC (insets: the corresponding S-V plots), respectively. (b) and (d) The detection limit calculation of **LCU-128** toward TC in NaCl and Na_2SO_4 solutions, respectively.

Fig. S9 (a) PXRD spectra of **LCU-128** after soaking in aqueous solution of TC. (b) Excitation and emission spectra of **LCU-128** and UV-vis absorption spectra of antibiotic solutions (10^{-4} M).

Fig. S10 (a) Fluorescence lifetimes of **LCU-128** in the presence and absence of TC. (b) HOMO and LUMO energy levels for H_3L and TC.

Fig. S11 (a)-(d) XPS spectra of **LCU-128** before and after immersion in TC and high resolution regions of Cd3d, N1s and O1s.

Fig. S12 Time-dependent intensity of **LCU-127** toward Tb^{3+} at 545 nm.

Fig. S13 Luminescence intensity of **LCU-127** in Ln^{3+} aqueous solutions with or without Tb^{3+} at 545 nm.

Fig. S14 PXRD spectra of **LCU-127** after soaking in aqueous solution of Tb^{3+}.

Fig. S15 (a) and (b) SEM images of **LCU-127** before and after immersing in 10^{-3} M Tb^{3+} aqueous solutions for three days, respectively.

Fig. S16 EDS mapping of **LCU-127** after immersing in 10^{-3} M Tb^{3+} aqueous solutions for three days.

Fig. S17 (a) Luminescence lifetime curves of **LCU-127**, **Tb^{3+}+LCU-127** and **Tb^{3+}+LCU-127** in OTC aqueous solutions. (b) The photographs of **LCU-127** in different solutions under 254 nm UV lamp (1: **LCU-127**-H_2O; 2: **LCU-127-**Tb^{3+}; 3: **Tb^{3+}+LCU-127**-TC, 4: **Tb^{3+}+LCU-127**-OTC)).

Fig. S18 (a) Time-dependent response of **Tb^{3+}+LCU-127** toward OTC. (b) The recycling experiment of **Tb^{3+}+LCU-127** toward OTC within five runs.

Fig. S19 (a)-(g) Luminescence intensity of **Tb^{3+}+LCU-127** in NaCl, Na_2SO_4 solutions, at 0 °C and room temperature (25 °C) as well as in aqueous solutions with pH value of 5, 6, 8, and 9, respectively.

Fig. S20 (a) and (c) Emission spectra of **Tb^{3+}+LCU-127** dispersed in NaCl and Na_2SO_4 solutions upon incremental addition of OTC (insets: the corresponding S-V plots), respectively. (b) and (d) The detection limit calculation of **Tb^{3+}+LCU-127** toward OTC in NaCl and Na_2SO_4 solutions, respectively.

Fig. S21 (a) and (c) XRD patterns and SEM image of MMM based on **Tb^{3+}+LCU-127**. (b) and (d) XRD patterns and SEM image of MMM based on **LCU-128**.

Materials and characterization.

The reagents used in the experiment include Tetrahydrofuran (THF), Methanol (MeOH), Ethanol (EtOH), N,N-Dimethylformamide (DMF), N,N-Dimethylacetamide (DMA), Dichloromethane (CH_2Cl_2), acetone, Acetonitrile (CH_3CN), Ethyl acetate (EA), Dimethyl sulfoxide (DMSO), 4-Aminophenol (4-Ap), 3-Aminophenol (3-Ap), *o*-Phenylenediamine (*o*-PD), *m*-Phenylenediamine (*m*-PD). 4-(3,5-dicarboxylatobenz-yloxy) benzoic acid (H_3L) and1,3,5-tris(1,2,4-tiazol-1-ylmethyl)-2,4,6-trimethylbenz-ene (ttytb) and 2,4,6-tris(4-pyridyl)-1,3,5-triazine(tpytz) were purchased from Jinan Henghua. Other reagents (A. R. grade) were commercially purchased and used as received without further purification. Powder X-ray diffraction (PXRD) data were collected over the 2θ range of 5–50° using a SmartLab diffractometer with Cu Kα radiation (λ = 1.5418 Å) at room temperature. Thermal analyses were performed on STA 449 F5 Jupiter instrument from room temperature to 800 °C with a heating rate of 10 °C/min under flowing nitrogen. Luminescence sensing properties were recorded on the Hitachi F-7000 Luminescence spectrophotometer. X-ray photoelectron spectroscopy (XPS) characterization was carried out by using a Thermo Fisher Scientific ESCALAB Xi+ spectrometer with Al Kα X-rays (1486.6 eV) as the light source and C 1s at 284.8 eV was used as a reference for all the all binding energies. UV-vis measurements were conducted with a UH 4150 spectrophotometer.

X-ray crystallographic study.

Single crystal X-ray diffraction data of **LCU-127** was collected on a Siemens Smart CCD diffractometer with graphite-monochromatic Mo Kα radiation (λ = 0.71073 Å) at 293(2) K. Single crystal X-ray diffraction data of **LCU-128** was collected with an Agilent Xcalibur Eos Gemini CCD diffractometer at 293(2) K with Cu Kα radiation (λ = 1.54184 Å). Both structures were solved by direct method and refined by full matrix least-squares technique. Nonhydrogen atoms are refined by anisotropic temperature parameters. The hydrogen atoms of carbon and oxygen atoms were placed in the calculated positions using isotropic thermal displacement parameters. Combined with the results of TG and elemental analysis, the SQUEEZE command was carried out to calculate the number of lattice water and DMF molecules because the positions of solvent molecules cannot be located from the diffraction peak. The CCDC number for **LCU-127** and **LCU-128** are 2363067 and 2363068.

Sensing antibiotics.

2 mg of ground samples (**LCU-127** and **LCU-128**) were added to 3.0 mL of solutions containing antibiotics (10^{-4} M, tetracycline (TC), chlortetracycline (CTC), oxytetracycline (OTC), ampicillin (AMP), erythromycin (EM), metronidazole (MDZ), ornidazole (ODZ), ronidazole (RDZ), nitrofurantoin (NFT), nitrofurazone (NZF), sulfadiazine (SDZ), sulfamethazine (SMZ), and thiamphenicol (TAP)) to form stable suspensions after ultrasounded for 30 minutes.

Sensing cations.

2 mg of ground samples of **LCU-127** and **LCU-128** were added to 3.0 mL aqueous solutions (10^{-3} M) of different metal salts ($Eu(NO_3)_3·6H_2O$, $Tb(NO_3)_3·6H_2O$, $Sm(NO_3)_3·6H_2O$, $Gd(NO_3)_3·5H_2O$, $La(NO_3)_3·6H_2O$, $Ce(NO_3)_3·6H_2O$, $Nd(NO_3)_3·6H_2O$, $HoCl_3·6H_2O$, $Er(NO_3)_3·5H_2O$, $Pr(NO_3)_3·5H_2O$, $Tm(NO_3)_3·5H_2O$, $Yb(NO_3)_3·6H_2O$, $Lu(NO_3)_3·6H_2O$, and $Dy(NO_3)_3·6H_2O$, forming stable suspensions after ultrasounded for 30 minutes.

Titration, anti-interference and recycling experiments.

The titration experiments were carried out as follows: Different amount of Tb^{3+} (10^{-3} M) or TC (10^{-4} M) was added to the suspensions of **LCU-127** or **LCU-128** (2 mg/3.0 mL). For OTC, 2 mg well ground **LCU-127** samples were dispersed in a solution of Tb^{3+} (10^{-3} M, 1.0 mL), and different amount of OTC solution (10^{-4} M) was added gradually.

The anti-interference experiment of **LCU-127** toward Tb^{3+} was performed as below: Tb^{3+} (10^{-3} M, 1.5 mL) and other metal ions (10^{-3} M, 1.5 mL) were mixed to form suspensions with well ground sample of **LCU-127** (2 mg). In the experiment of **LCU-128** toward TC, a solution of TC (2×10^{-4} M, 1.5 mL) was mixed with other antibiotics (2×10^{-4} M, 1.5 mL), common cations (nitrate salt of NH_4^+, Al^{3+}, Mg^{2+}, Na^+, Cu^{2+}, Ca^{2+}, K^+, 1×10^{-3} M, 1.5 mL), anions (sodium salt of CO_3^{2-}, NO_3^-, OH^-, SO_4^{2-}, Cl^-, 1×10^{-3} M, 1.5 mL), organic matters (EtOH, DMF, CH_2Cl_2, CH_3CN, EA, DMSO, acetone, 1.5 mL) or aqueous solutions of 4-Ap, 3-Ap, *o*-PD, *m*-PD (1×10^{-3} M, 1.5 mL). Well ground samples of **LCU-128** (2 mg) were dispersed into the aftermentioned solutions to form stable suspensions.

In the recycling experiment, the samples after sensing were collected by centrifugation and cleaned thoroughly with H_2O (for TC) or $Tb(NO_3)_3$ solution (for OTC) for re-measurement.

Calculation of the HOMO and LUMO.

The HOMO and LUMO energy levels were calculated at the B3PW91/6-31G accuracy level by density functional theory (DFT), using the Gaussian 09 package of programs. The harmonic frequency was calculated to make sure that the acquired structure was the local minimum. Gaussian 09, Revision B.01, M. J. Frisch, G. W. Trucks, H. B. Schlegel, G. E. Scuseria, M. A. Robb, J. R. Cheeseman, G. Scalmani, V. Barone, B. Mennucci, G. A. Petersson, H. Nakatsuji, M. Caricato, X. Li, H. P. Hratchian, A. F. Izmaylov, J. Bloino, G. Zheng, J. L. Sonnenberg, M. Hada, M. Ehara, K. Toyota, R. Fukuda, J. Hasegawa, M. Ishida, T. Nakajima, Y. Honda, O. Kitao, H. Nakai, T. Vreven, J. A. Montgomery, Jr., J. E. Peralta, F. Ogliaro, M. Bearpark, J. J. Heyd, E. Brothers, K. N. Kudin, V. N. Staroverov, T. Keith, R. Kobayashi, J. Normand, K. Raghavachari, A. Rendell, J. C. Burant, S. S. Iyengar, J. Tomasi, M. Cossi, N. Rega, J. M. Millam, M. Klene, J. E. Knox, J. B. Cross, V. Bakken, C. Adamo, J. Jaramillo, R. Gomperts, R. E. Stratmann, O. Yazyev, A. J. Austin, R. Cammi, C. Pomelli, J. W. Ochterski, R. L. Martin, K. Morokuma, V. G. Zakrzewski, G. A. Voth, P. Salvador, J. J. Dannenberg, S. Dapprich, A. D. Daniels, O. Farkas, J. B. Foresman, J. V. Ortiz, J. Cioslowski, and D. J. Fox, Gaussian, Inc., Wallingford CT, 2010.

Table S1 Crystal structure data and refinement parameters of **LCU-127** and **LCU-128**.

Compound	**LCU-127**	**LCU-128**
Formula	$C_{37}H_{44}CdN_{10}O_{11}$	$C_{34}H_{23}CdN_6O_8$
Formula weight	917.22	755.99
T [K]	293(2)	293(2)
Crystal system	Triclinic	Triclinic
Space group	P-1	P-1
a [Å]	10.1521(11)	10.1731(5)
b [Å]	13.6394(13)	11.7031(7)
c [Å]	15.1144(14)	13.1709(7)
α [˚]	103.171(3)	85.370(5)
β [˚]	99.798(2)	89.565(4)
γ [˚]	101.474(3)	76.003(5)
V [Å^3]	1945.5(3)	1516.45(15)
Z	2	2
$D_{calcd.}$ [g·cm^{-3}]	1.349	1.656
μ [mm^{-1}]	0.616	6.336
θ range	2.101-25.02	3.367-67.248
index ranges	-12≤h≤12 -7≤k≤16 -17≤l≤17	-12≤h≤11 -13≤k≤13 -13≤l≤15
R1; wR_{2a} [I > 2σ(I)]	0.0532; 0.1444	0.0382; 0.0876
GOF	1.090	1.020

$^aR_1 = \Sigma| |F_o|-|F_c| | / \Sigma|F_o|$, $^bwR_2 = [\Sigma w(F_o^2-F_c^2)^2]/ \Sigma w(F_o^2)^2]^{1/2}$

Table S2 Selected bond lengths [Å] and angles [º] for **LCU-127** and **LCU-128**.

LCU-127			
Cd(1)-O(1)	2.597(4)	Cd(1)-O(2)	2.297(3)
Cd(1)-O(3A)	2.578(3)	Cd(1)-O(4A)	2.341(3)
Cd(1)-N(1)	2.333(4)	Cd(1)-N(5B)	2.332(4)
Cd(1)-N(9C)	2.375(4)	O(2)-Cd(1)-O(1)	52.54(12)
O(2)-Cd(1)-O(3A)	136.02(12)	O(2)-Cd(1)-O(4A)	84.54(11)
O(2)-Cd(1)-N(1)	126.78(13)	O(2)-Cd(1)-N(5B)	89.87(14)
O(4A)-Cd(1)-O(1)	129.83(11)	O(4A)-Cd(1)-N(9C)	89.43(13)
N(1)-Cd(1)-O(1)	81.15(13)	N(1)-Cd(1)-O(3A)	95.43(13)
N(1)-Cd(1)-O(4A)	147.92(13)	N(1)-Cd(1)-N(9C)	86.52(15)
N(5B)-Cd(1)-O(4A)	89.26(12)	N(5B)-Cd(1)-N(1)	84.62(14)
N(9C)-Cd(1)-O(1)	82.71(14)	N(9C)-Cd(1)-O(3A)	82.65(13)
LCU-128			
Cd(1)-O(1)	2.270(3)	Cd(1)-O(3B)	2.376(3)
Cd(1)-O(4B)	2.487(3)	Cd(1)-O(8)	2.374(3)
Cd(1)-N(1)	2.337(3)	Cd(1)-N(6A)	2.349(3)
N(1)-Cd(1)-N(6A)	101.13(12)	N(1)-Cd(1)-O(3B)	86.98(11)
N(1)-Cd(1)-O(4B)	138.98(11)	N(1)-Cd(1)-O(8)	84.66(11)
N(6A)-Cd(1)-O(3B)	96.96(12)	N(6A)-Cd(1)-O(4B)	93.27(12)
N(6A)-Cd(1)-O(8)	171.09(10)	O(8)-Cd(1)-O(4B)	86.56(10)
O(1)-Cd(1)-N(6A)	88.15(11)	O(1)-Cd(1)-O(3B)	133.78(11)
O(1)-Cd(1)-O(4B)	80.92(10)	O(1)-Cd(1)-O(8)	83.03(10)
O(3B)-Cd(1)-O(4B)	53.00(10)	O(8)-Cd(1)-O(3B)	90.05(11)

Symmetry codes: LCU-127: A:1+x,+y,+z; B: 2-x,1-y,2-z; C: 2-x,1-y,1-z; **LCU-128**: A:+x,+y,-1+z; B: 1+x,+y,+z.

Table S3 The reported CPs/MOFs as sensors for TC detection.

Luminescent material	Detection mechanism	Detection limit	Reference
Eu-L	turn off	0.43 μM	3
LCU-123	turn off	0.552 μM	54
ZIF-8@SA	turn on	58.46 nM	56
Eu:Tb-CP	turn on	0.1498 μM	57
Laponite-Eu-Cit	turn on	9.5 nM	58
$\{[Cd(2\text{-}F\text{-}tzba)(H_2O)]\cdot 1.5H_2O\}_n$	turn off	8.97 mmol L^{-1}	59
$\{[Cd(3\text{-}F\text{-}tzba)(H_2O)]\cdot 1.5H_2O\}_n$	turn off	9.39 mmol L^{-1}	59
$\{[Zn(bdc)(4,4'\text{-}bidpe)]\cdot H_2O\}_n$	turn off	3.72×10^{-7} M	60
LCU-127	turn off	0.18 μM	this work

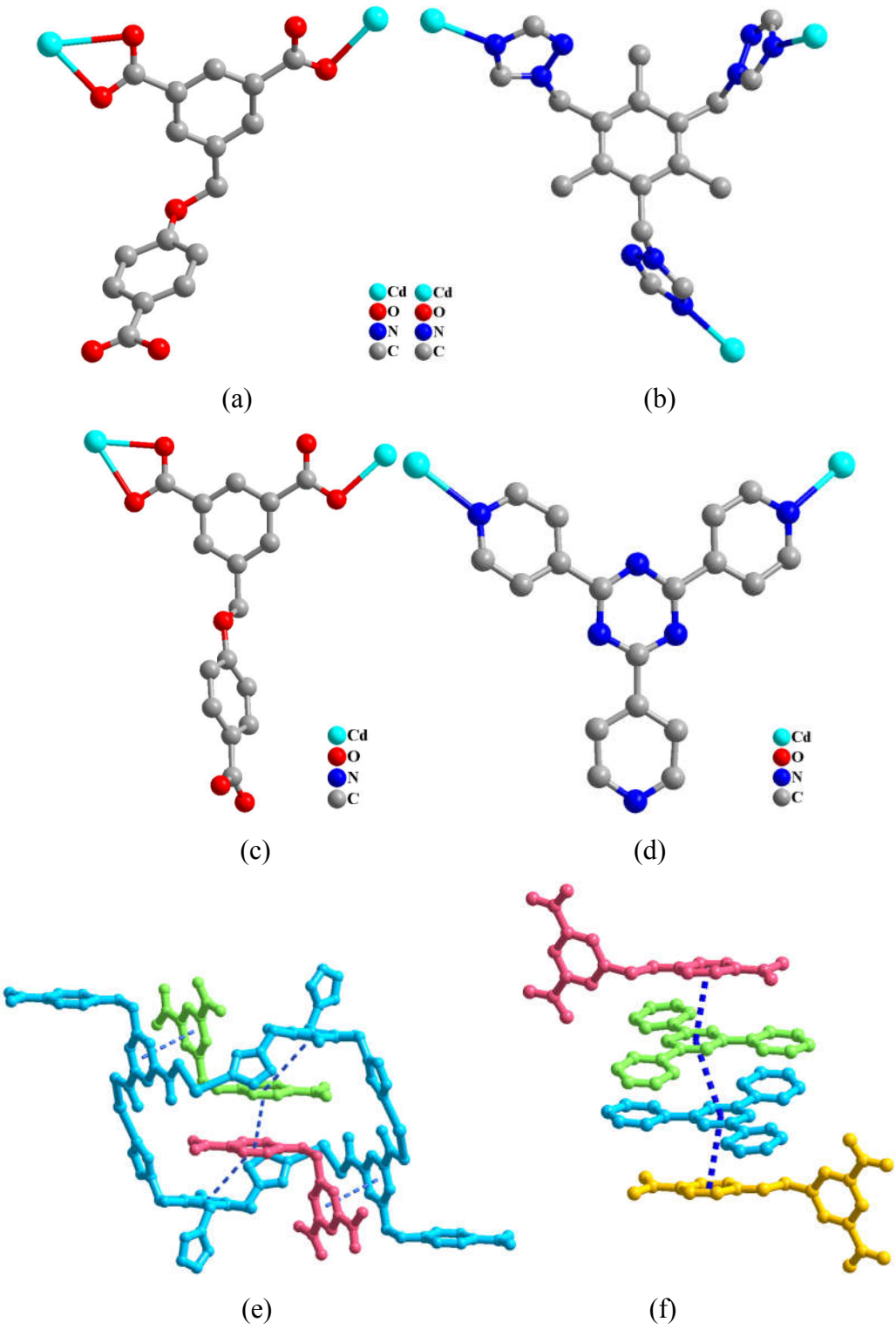

Fig. S1 (a) and (c) Coordination mode of H_3L in **LCU-127** and **LCU-128**, respectively. (b) and (d) Coordination mode of ttytb and tpytz in **LCU-127** and **LCU-128**, respectively. (e) and (f) Stacking interactions of **LCU-127** and **LCU-128** between adjacent layers, respectively.

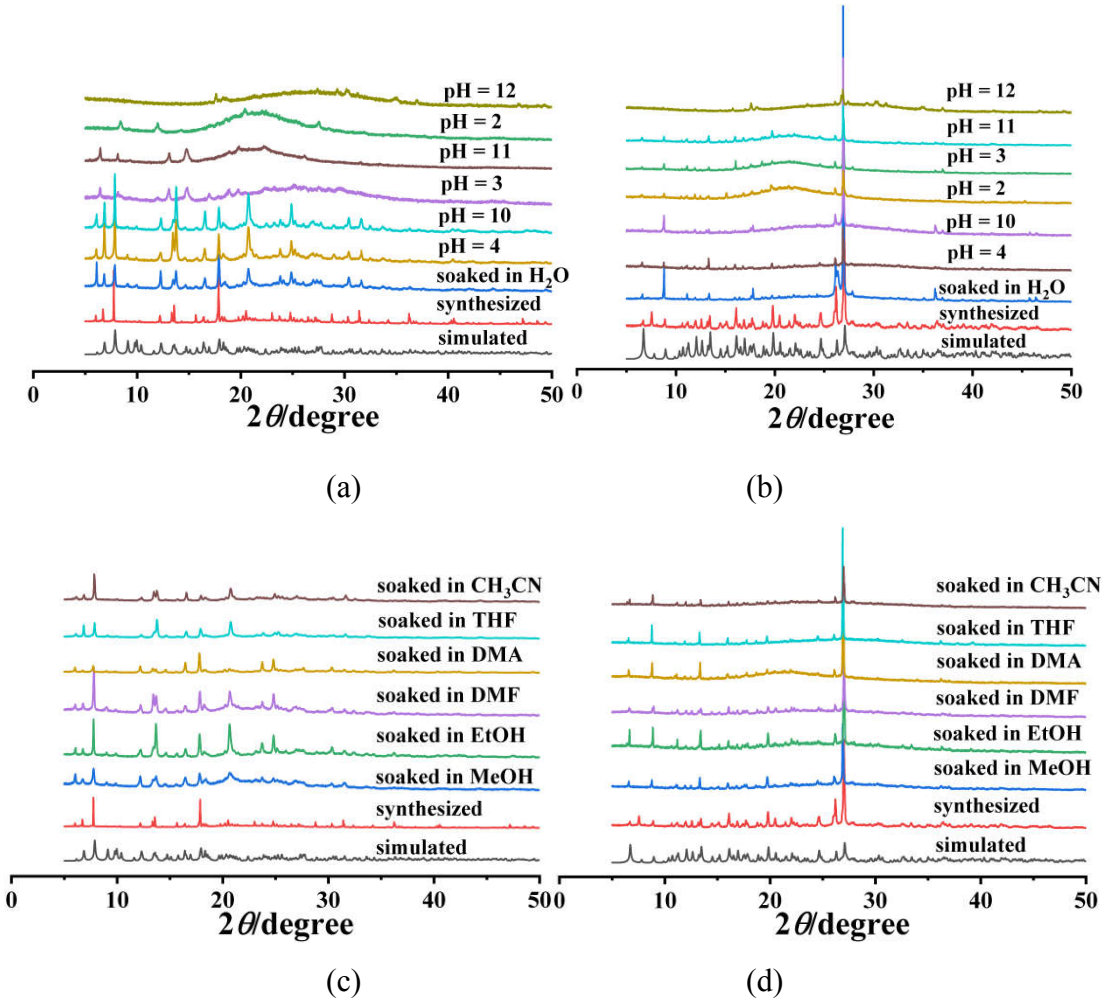

Fig. S2 (a) and (b) PXRD spectra of **LCU-127** and **LCU-128** after soaking in H_2O and different pH solutions, respectively**.** (c) and (d) PXRD spectra of **LCU-127** and **LCU-128** after soaking in different organic solvents for three days, respectively.

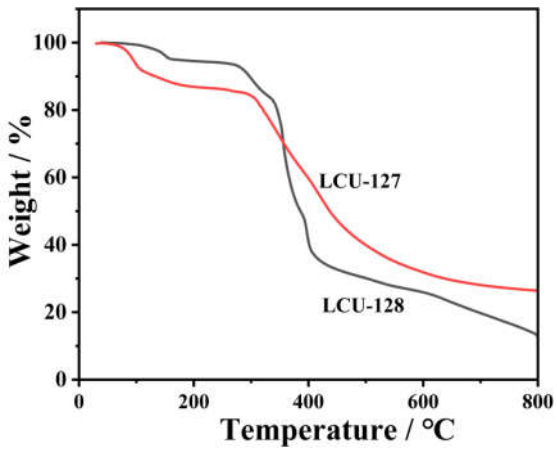

Fig. S3 TG of **LCU-127** and **LCU-128**, respectively.

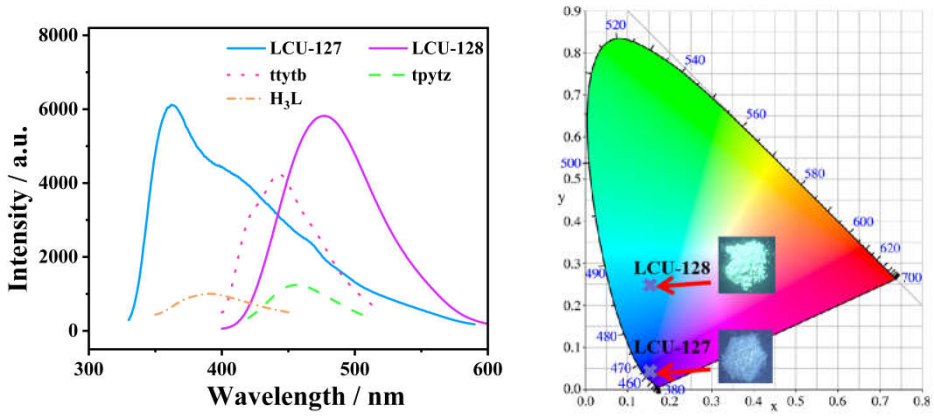

(a) (b)

Fig. S4 (a) Solid-state emission spectra and (b) CIE coordinates of **LCU-127** and **LCU-128**.

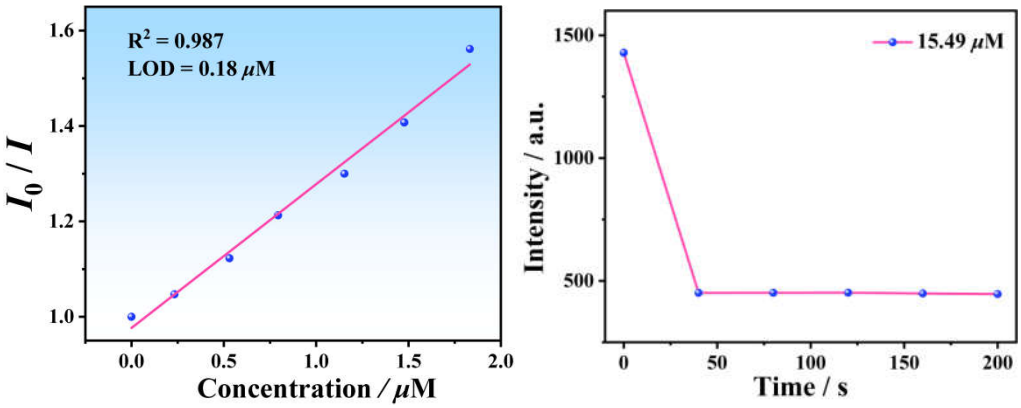

(a) (b)

Fig. S5 (a) The detection limit calculation and (b) time-dependent response of **LCU-128** toward TC.

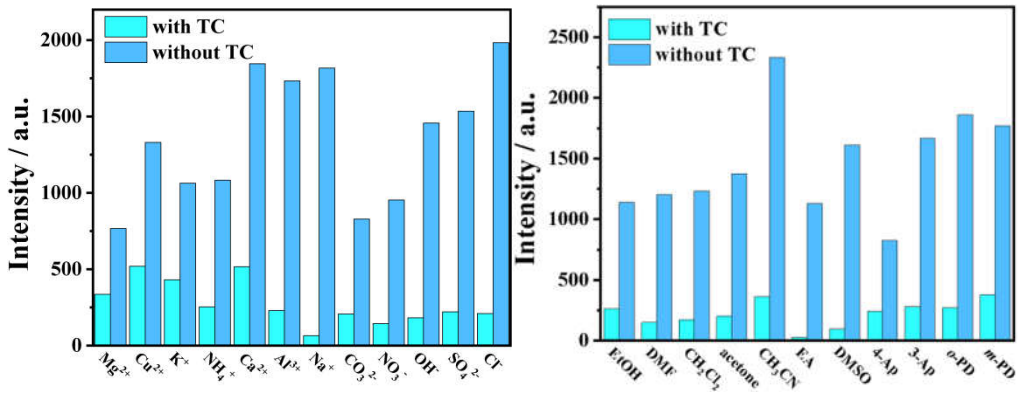

(a) (b)

Fig. S6 (a) and (b) The luminescence intensity of **LCU-128** suspensions of common cations, anions, and some common organic matters with and without TC, respectively.

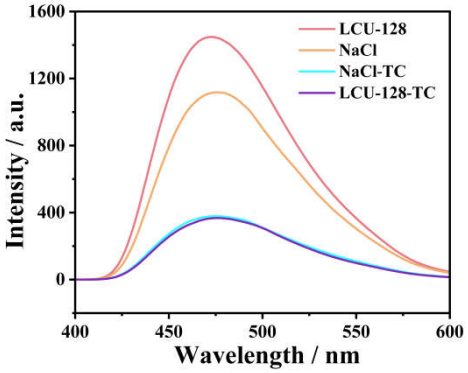
LCU-128
NaCl
NaCl-TC
LCU-128-TC
Intensity / a.u.
Wavelength / nm

(a)

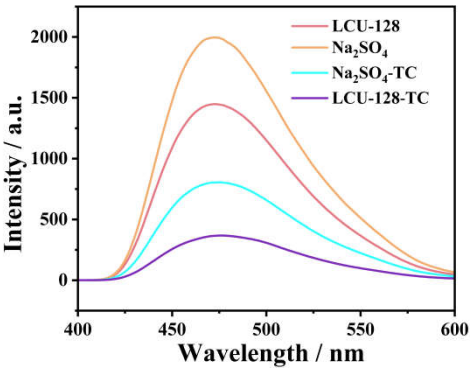
LCU-128
Na2SO4
Na2SO4-TC
LCU-128-TC
Intensity / a.u.
Wavelength / nm

(b)

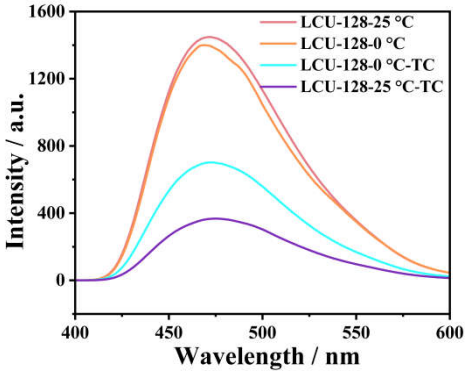
LCU-128-25 °C
LCU-128-0 °C
LCU-128-0 °C-TC
LCU-128-25 °C-TC
Intensity / a.u.
Wavelength / nm

(c)

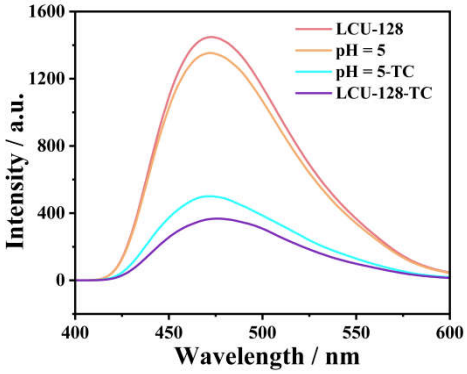
LCU-128
pH = 5
pH = 5-TC
LCU-128-TC
Intensity / a.u.
Wavelength / nm

(d)

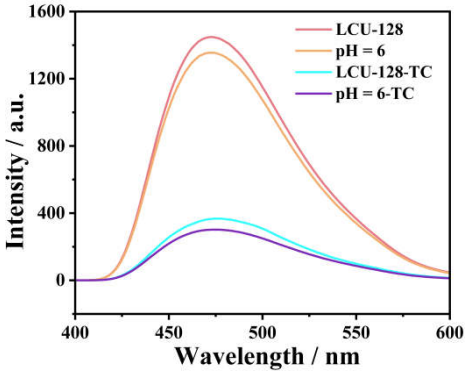
LCU-128
pH = 6
LCU-128-TC
pH = 6-TC
Intensity / a.u.
Wavelength / nm

(e)

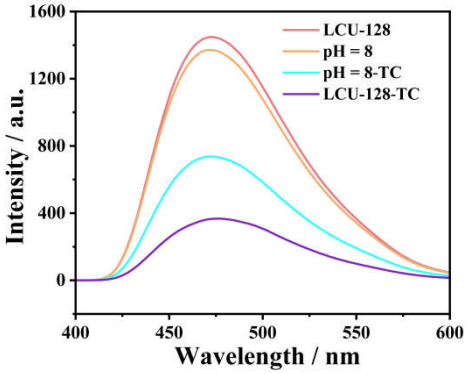
LCU-128
pH = 8
pH = 8-TC
LCU-128-TC
Intensity / a.u.
Wavelength / nm

(f)

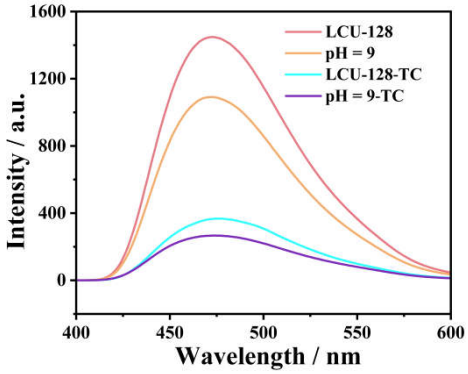
LCU-128
pH = 9
LCU-128-TC
pH = 9-TC
Intensity / a.u.
Wavelength / nm

(g)

Fig. S7 (a)-(g) Luminescence intensity of **LCU-128** toward TC in NaCl, Na_2SO_4 solutions, temperature at 0 °C and room temperature (25 °C) and pH at 5, 6, 8, and 9, respectively.

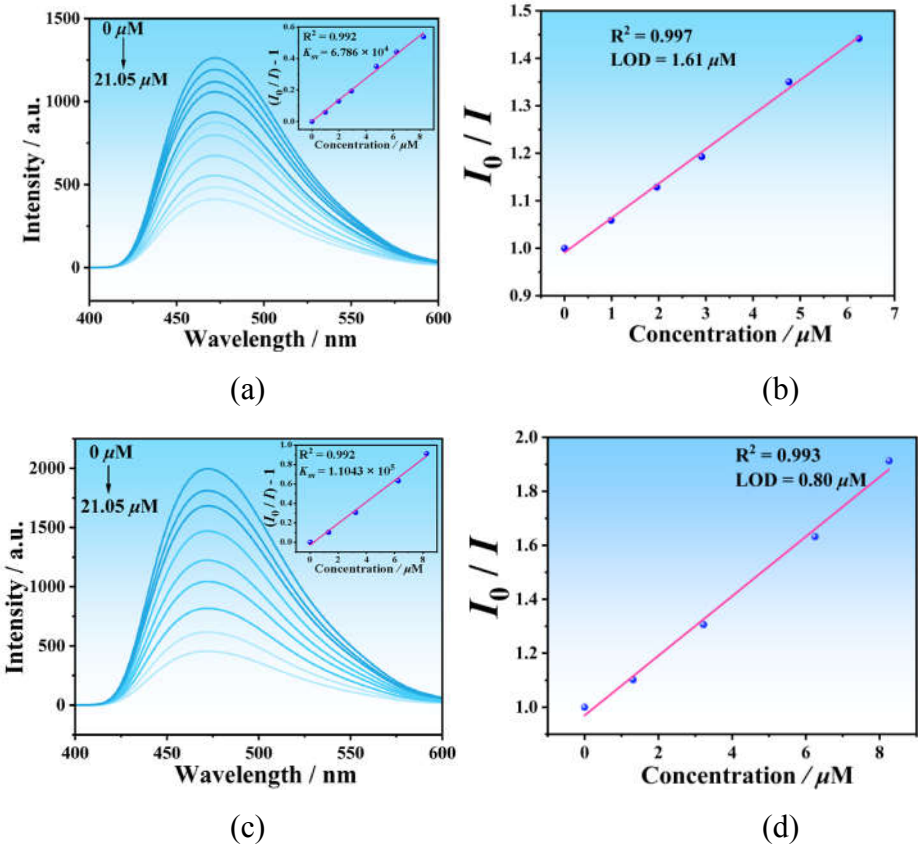

Fig. S8 (a) and (c) Emission spectra of **LCU-128** dispersed in NaCl and Na_2SO_4 upon incremental addition of TC (insets: the corresponding S-V plots), respectively. (b) and (d) The detection limit calculation of **LCU-128** toward TC in NaCl and Na_2SO_4 solutions, respectively.

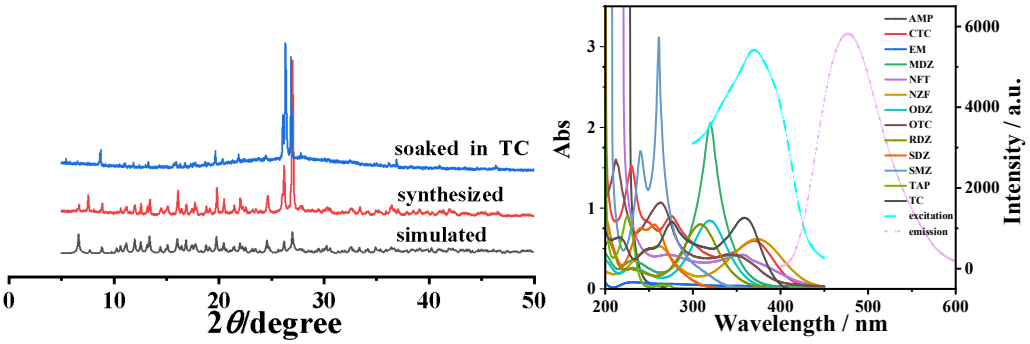

Fig. S9 (a) PXRD spectra of **LCU-128** after soaking in aqueous solution of TC. (b) Excitation and emission spectra of **LCU-128** and UV-vis absorption spectra of antibiotic solutions (10^{-4} M).

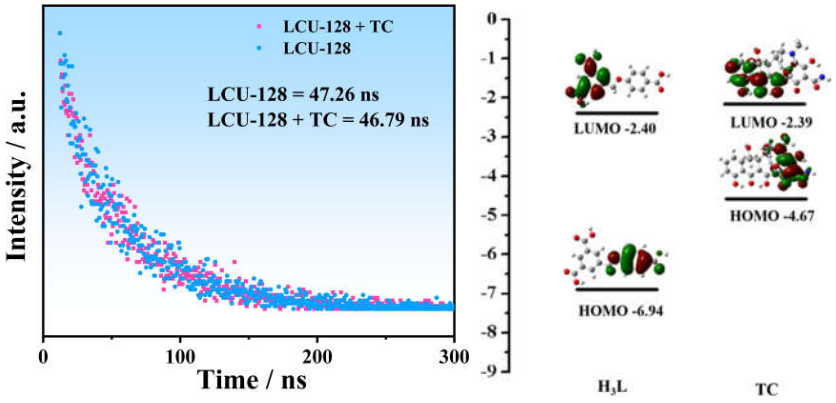

(a) (b)

Fig. S10 (a) Fluorescence lifetimes of **LCU-128** in the presence and absence of TC. (b) HOMO and LUMO energy levels for H_3L and TC.

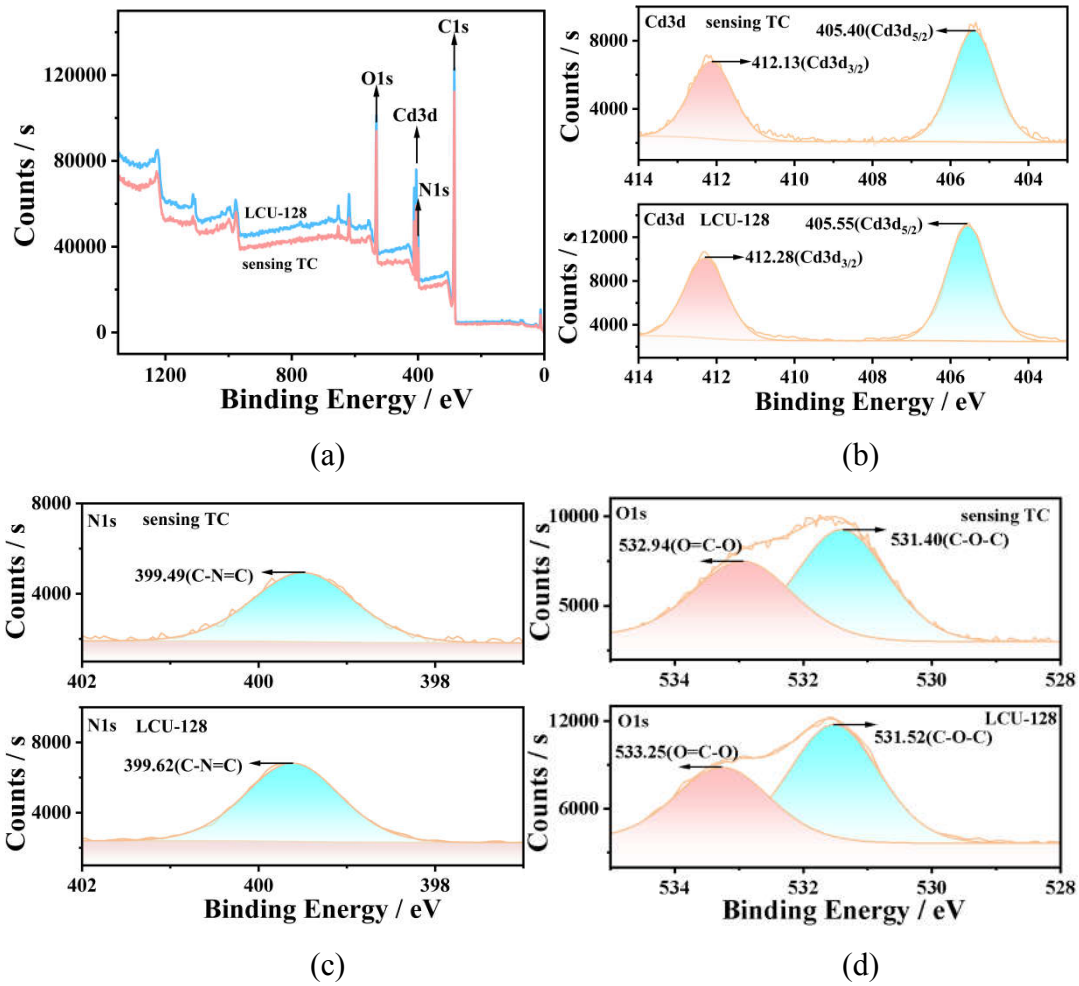

(a) (b)

(c) (d)

Fig. S11 (a)-(d) XPS spectra of **LCU-128** before and after immersion in TC and high resolution regions of Cd3d, N1s and O1s.

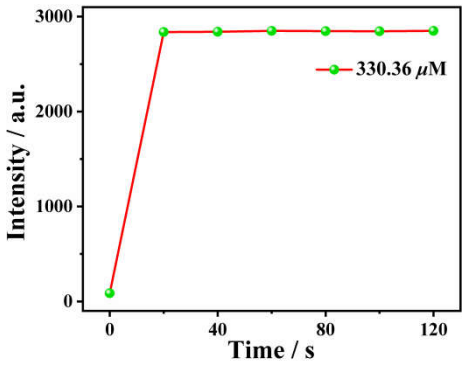

Fig. S12 Time-dependent intensity of **LCU-127** toward Tb^{3+} at 545 nm.

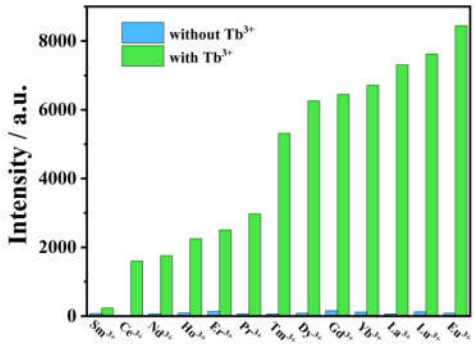

Fig. S13 Luminescence intensity of **LCU-127** in Ln^{3+} aqueous solutions with or without Tb^{3+} at 545 nm.

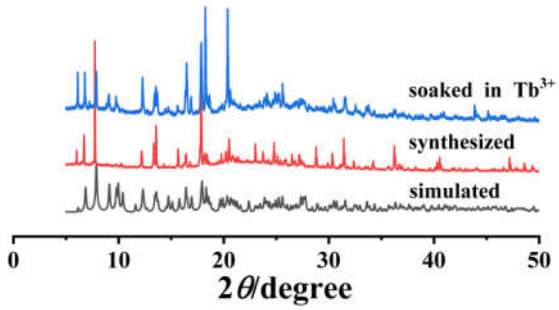

Fig. S14 PXRD spectra of **LCU-127** after soaking in aqueous solution of Tb^{3+}.

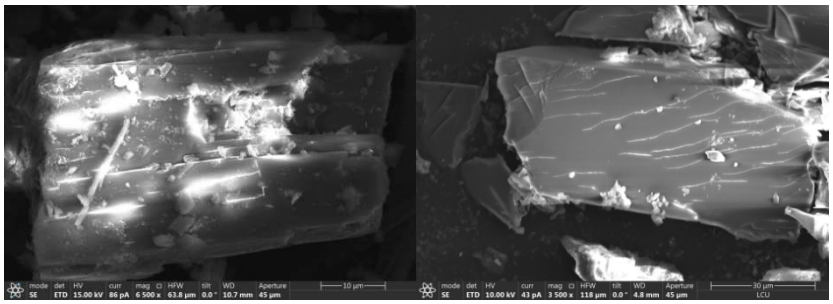

(a) (b)

Fig. S15 (a) and (b) SEM images of **LCU-127** before and after immersing in 10^{-3} M Tb^{3+} aqueous solutions for three days, respectively.

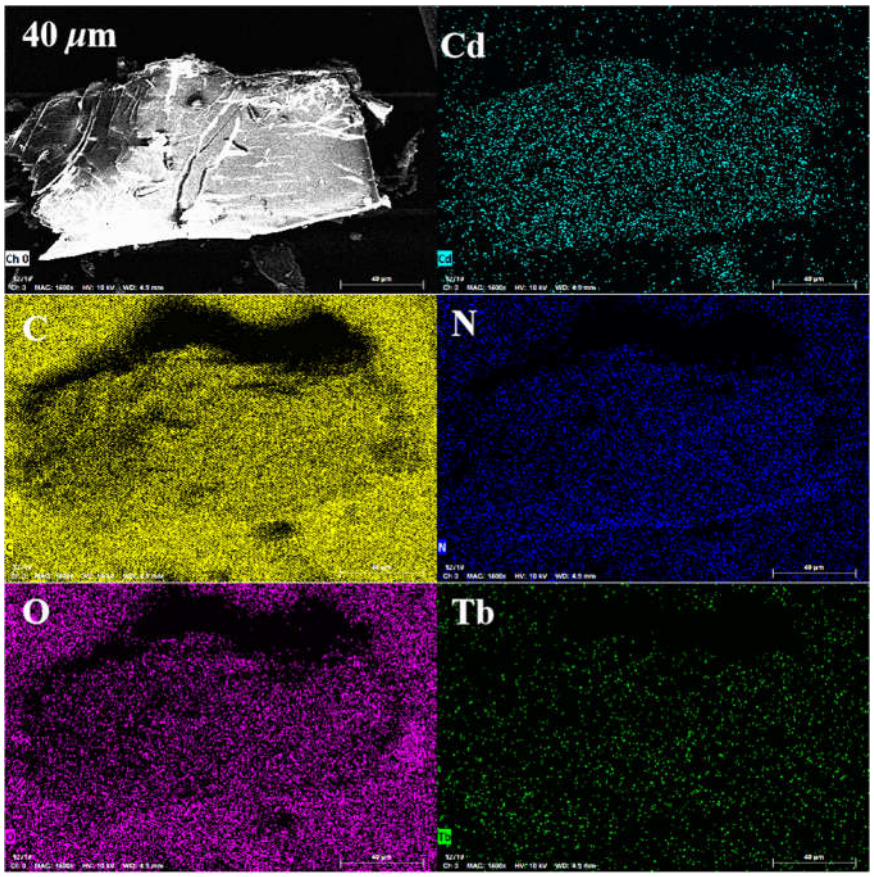

Fig. S16 EDS mapping of **LCU-127** after immersing in 10^{-3} M Tb^{3+} aqueous solutions for three days.

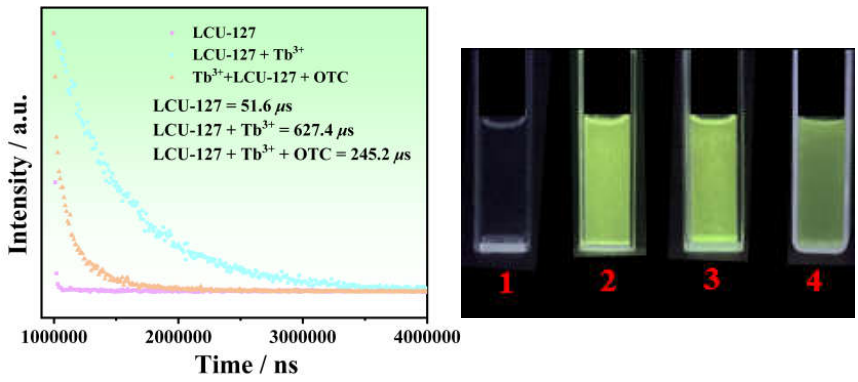

(a) (b)

Fig. S17 (a) Luminescence lifetime curves of **LCU-127**, **Tb^{3+}+LCU-127** and **Tb^{3+}+LCU-127** in OTC aqueous solutions. (b) The photographs of **LCU-127** in different solutions under 254 nm UV lamp (1: **LCU-127**-H_2O; 2: **LCU-127**-Tb^{3+}; 3: **Tb^{3+}+LCU-127**-TC, 4: **Tb^{3+}+LCU-127**-OTC)).

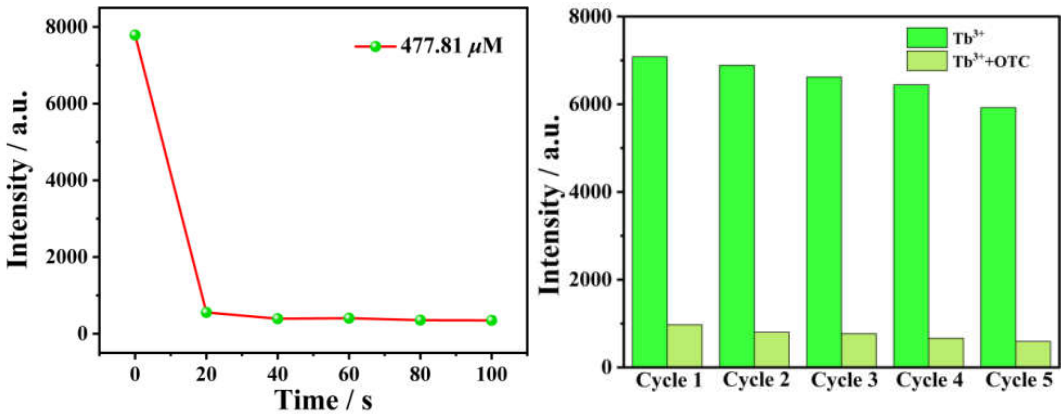

(a) (b)

Fig. S18 (a) Time-dependent response of **Tb^{3+}+LCU-127** toward OTC. (b) The recycling experiment of **Tb^{3+}+LCU-127** toward OTC within five runs.

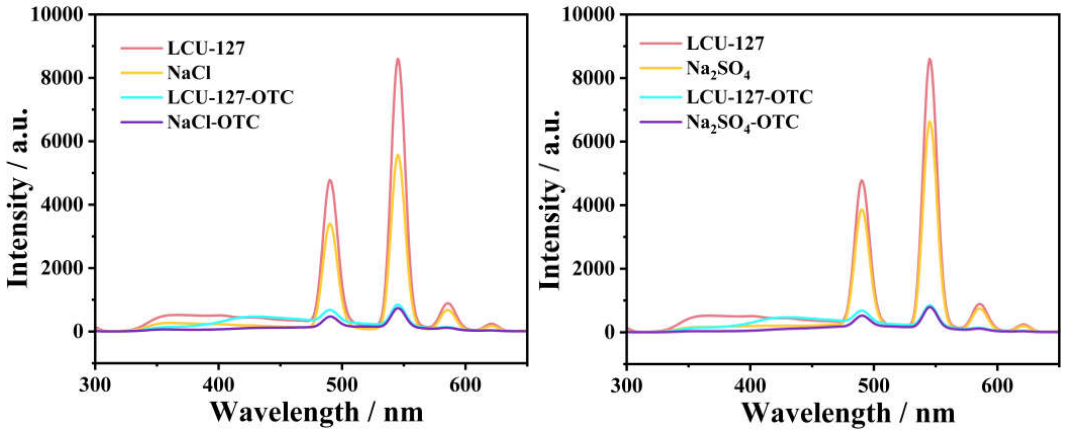

(a) (b)

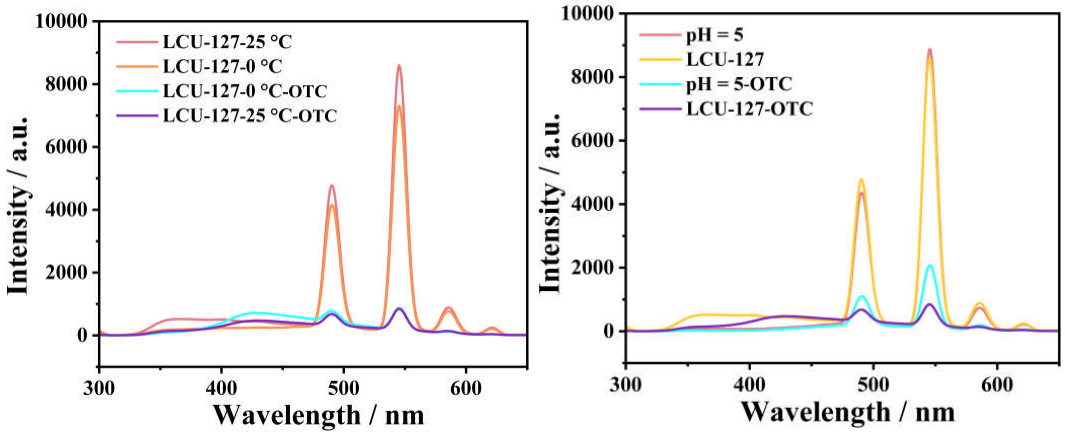

(c) (d)

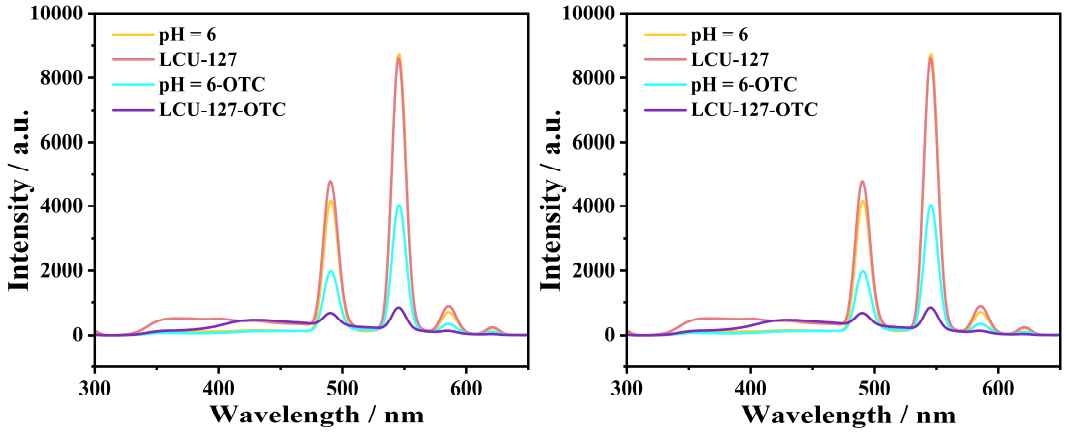

(e) (f)

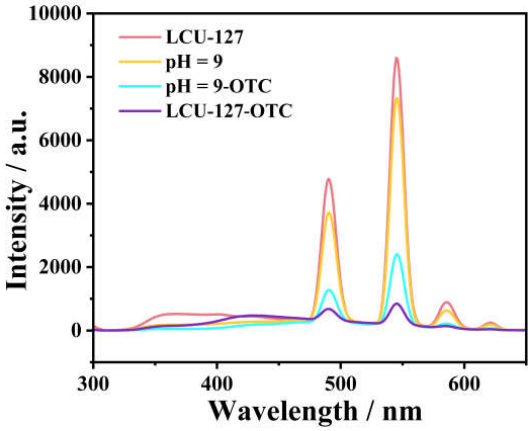

(g)

Fig. S19 (a)-(g) Luminescence intensity of **Tb^{3+}+LCU-127** in NaCl, Na_2SO_4 solutions, at 0 °C and room temperature (25 °C) as well as in aqueous solutions with pH value of 5, 6, 8, and 9, respectively.

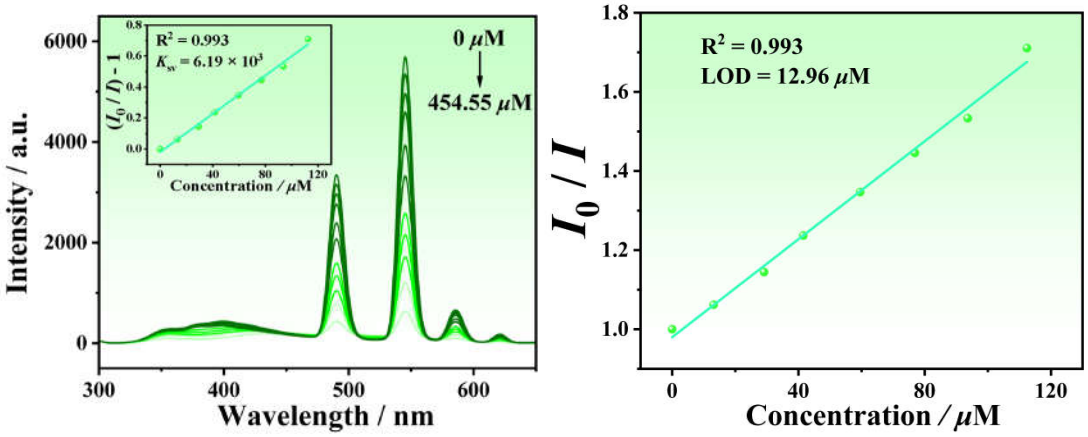

(a) (b)

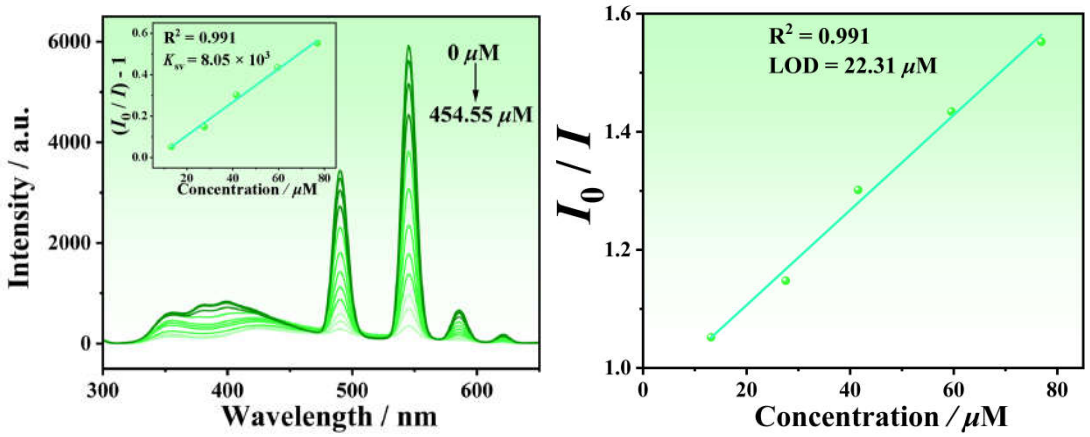

(c) (d)

Fig. S20 (a) and (c) Emission spectra of **Tb^{3+}+LCU-127** dispersed in NaCl and Na_2SO_4 solutions upon incremental addition of OTC (insets: the corresponding S-V plots), respectively. (b) and (d) The detection limit calculation of **Tb^{3+}+LCU-127** toward OTC in NaCl and Na_2SO_4 solutions, respectively.

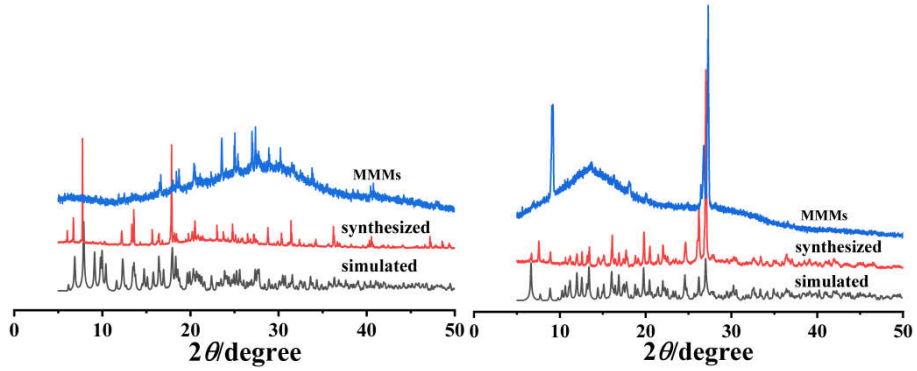

(a) (b)

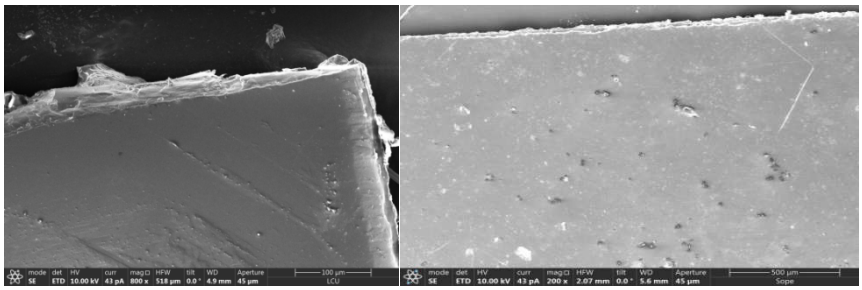

(c) (d)

Fig. S21 (a) and (c) XRD patterns and SEM image of MMM based on **Tb^{3+}+LCU-127**. (b) and (d) XRD patterns and SEM image of MMM based on **LCU-128**.